Advances in Astronautics Science and Technology (2020) 3:157–163
https://doi.org/10.1007/s42423-020-00062-1

ORIGINAL PAPER

Development of Micro-radioisotope Thermoelectric Power Supply for Deep Space Exploration Distributed Wireless Sensor Network

Zicheng Yuan[1] · Kai Liu[1] · Zhiheng Xu[1] · Hongyu Wang[1] · Yunpeng Liu[1] · Xiaobin Tang[1]

Received: 11 October 2019 / Revised: 23 October 2020 / Accepted: 27 October 2020 / Published online: 12 November 2020

Abstract

A radioisotope thermoelectric generator (RTG) is a device that directly converts the decay heat of a radioisotope into electrical energy using the Seebeck effect of a thermoelectric material. The constant decay of the radioisotope heat source produces heat as a system energy source. The thermoelectric module uses materials to obtain electric energy by Seebeck effect. The structure and size of the thermoelectric converter need to be optimized for different radioisotope heat sources. The power has stable output performance, sustainable operation, and strong environmental adaptability. Space micro-scientific instruments require power supplies that are sustainable, stable, and long-life. The micro radioisotope thermoelectric generator can be invoked as a sustainable long-life power supply in low-power device applications. The miniaturized RTG can be applied in long-term service meteorological/seismic monitoring stations that are widely distributed on the surface of the planet, small landing vehicles at extreme latitudes or areas with low solar flux, atmospheric-surface-flow monitoring systems, underground detectors, deep space micro spacecraft, wireless sensor networks, self-powered radiation sensors, deep-space robot probes, and radio observatories on the lunar surface. This study innovatively proposes micro stacked-integrated annular-radial radioisotope thermoelectric generator and prepares an integrated prototype to drive an RF2500-based radiofrequency wireless sensor network, and monitors the temperature of each node for a long time as a demonstration. A high-performance micro radioisotope thermoelectric generators module based on the flexible printed circuit and bismuth telluride thick film was designed and prepared by screen printing. They are tested by a loading electrically heated equivalent radioisotope heat source. The output performance of the micro-RTG at different ambient temperatures is further evaluated. When loaded with $^{238}PuO_2$ radioisotope heat sources, an integrated prototype would generate an open-circuit voltage of 0.815 V, a short-circuit current of 0.551 mA, and an output power of 114.38 μW at 0.408 V. When loaded with a $^{90}SrTiO_3$ or $^{241}AmO_2$ radioisotope heat source, the prototype produced 66.38% and 6.15% of the output power (compared to $^{238}PuO_2$), respectively. In the impact evaluation on ambient temperature, the electrical output performance of the prototype increases with increasing temperature (− 30 to 120 °C). In the evaluation of the effects of long-term radioisotope irradiation, the output performance decreased slightly as the irradiation dose was increased during the service period. The stack-integrated micro radioisotope thermoelectric generator developed in this study is expected to provide reliable power support for space micro-scientific instruments, especially distributed wireless sensor networks.

Keywords Radioisotope thermoelectric generator · Wireless sensor network · Micro energy · Long life battery · Deep space exploration

✉ Xiaobin Tang
tangxiaobin@nuaa.edu.cn

Zicheng Yuan
yuanzc@nuaa.edu.cn

Kai Liu
liukai-2015@nuaa.edu.cn

Zhiheng Xu
xuzhiheng@nuaa.edu.cn

Hongyu Wang
wanghongyu@nuaa.edu.cn

Yunpeng Liu
liuyp@nuaa.edu.cn

[1] Department of Nuclear Science and Technology, Nanjing University of Aeronautics and Astronautics, Nanjing 211106, China

1 Introduction

A radioisotope thermoelectric generator (RTG) is a device that directly converts the decay heat of a radioisotope into electrical energy using the Seebeck effect of a thermoelectric (TE) material. The constant decay of radioisotope heat source (e.g., ^{238}Pu and ^{90}Sr) produces heat as a system energy source. The TE module uses materials such as Bi_2Te_3, PbTe, SiGe, and skutterudite to obtain electric energy by the Seebeck effect. The structure and size of the TE converter need to be optimized for different radioisotope heat sources. The power has stable output performance, sustainable operation, and strong environmental adaptability [1–6]. The miniaturized RTG can be applied in long-term service meteorological/seismic monitoring stations that are widely distributed on the surface of the planet, small landing vehicles at extreme latitudes or areas with low solar flux, atmospheric-surface-flow monitoring systems, underground detectors [7], deep space micro spacecraft [8], wireless sensor networks [9], self-powered radiation sensors [10], deep-space robot probes [11], and radio observatories on the lunar surface [12].

Micro-RTGs consist of densely packed and small TE legs. However, developing micro-RTGs using bulk materials is challenging. Improving output performance in a limited space to increase conversion efficiency is the purpose of current studies. The advantages of this type of power supply with a small size and long life are still irreplaceable by other power sources [5, 13]. Thus, improving integration and performance is attracting the interest of many researchers [14, 15]. The manufacture of miniaturized and miniaturized devices is a difficult point that restricts the development and application of miniature RTGs. The miniaturized machine is often small in size and heat source. If the number of thermoelectric legs per unit volume is insufficient, it will result in a small temperature difference and low voltage, which is fatal to the load. To solve this problem, it is necessary to design the energy conversion structure, such as the annular thermoelectric energy conversion structure provided in this article, and at the same time integrate a large number of thermoelectric legs in the unit space. The screen printing process can produce dense thermoelectric legs and special structures cheaply, quickly, and in large quantities.

The structural design of TE legs and the printing process both have a decisive impact on the prototype performance. Based on the solid heat transfer simulation model, we optimized the number and size of the TE legs to obtain the proper voltage output [16]. We have also improved the printing process and curing temperature to improve the electrical conductivity and Seebeck coefficient of the TE material [17], thereby increasing the output power of the power unit [18]. In this work, we improve the electrical performance of a micro-RTG single module. The stack connection is also investigated, and the properties of series–parallel mode and the number of layers are explored. They are tested by a loading electrically heated equivalent radioisotope heat source. Energy-conversion efficiency is improved by fabricating space-stack TE devices. The output performance of the micro-RTG at different ambient temperatures is further evaluated.

Our research team completed multilayer prototype research and manufacturing, optimized the module components, and explored the coupling mechanism and influencing factors. Given the importance of the influence of environmental factors on the micro-RTG, the temperature effect of the 10-layer prototype was studied. The output of various stacking methods is also reported, and the load capacity as a power source is discussed. Through a highly integrated process, the micro-RTG can achieve higher voltage and power per unit volume and can thus meet the voltage and power requirements of various space components. This device is expected to solve fundamental technical problems in the field of space exploration.

2 Experimental

The thermoelectric structure is formed by a screen printing method. The printing thermoelectric ink materials are as follows, p-type Sb_2Te_3 and n-type $Bi_2Te_{2.7}Se_{0.3}$ 200 mesh powders are used as thermoelectric fillers, DER736 is the binder matrix, 4-MHHPA is the hardener, and 2E4MZ-CN is the accelerator. Among them, the equivalent weight ratio of epoxy and hardener is 1:0.85. Furthermore, use the 1-cyanoethyl-2-ethyl-4-methylimidazole (1.5 wt%; Shikoku Chemicals) as the catalyst in the system. The thermoelectric powder accounts for 80–85 wt% by weight in the ink.

The following steps are used to manufacture FPC-based thermoelectric modules in batches. First, print the P-legs, and then print the N-legs after the P-legs are dried. Next, it was cured at 90 °C for 30 min, and then the sample for device manufacturing was cut into circular slices and punched in the center. Finally, the batch-printed RTG modules were cured in N2 environment at 275 °C for 3 h.

The 10-layer prototype is composed of 10 single-layer modules stacked and welded, and the thermoelectric conversion principle of each layer is shown on Fig. 1. The single-layer module is reserved with two pads that can conduct electricity through the substrate. When stacking, the upper and lower adjacent discs are welded by solder. Following the principle that the positive electrode of the lower layer is aligned with the negative electrode of the upper layer, a 10-layer prototype can be connected in series. A single-layer module model is built using COMSOL Multiphysics software, meshing is performed according to the model volume microelement, and internal resistance is calculated using a

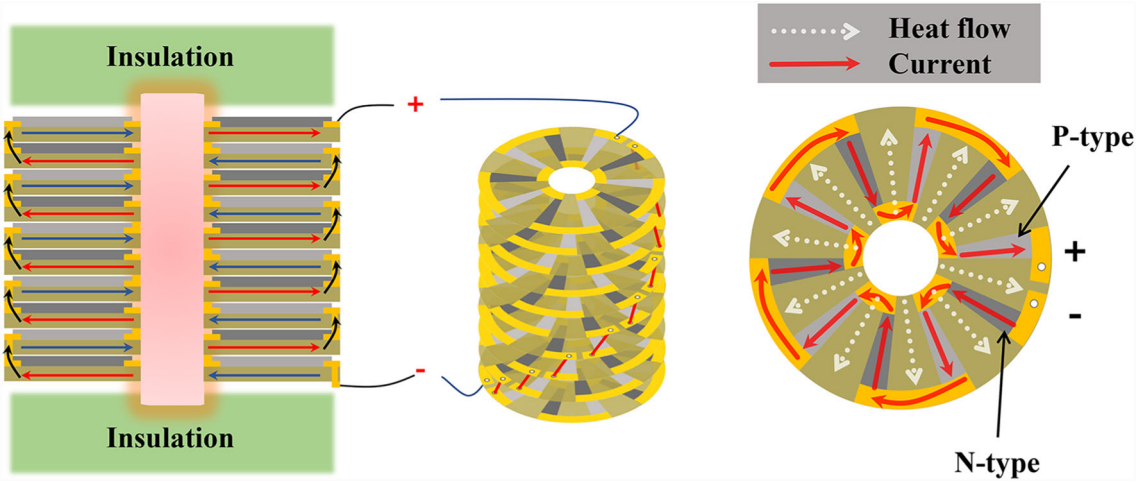

Fig. 1 Schematic diagram of the structure of a Micro-RTG

constant current. Given that the voltage source is linear, the internal resistance is the slope value of the I–V curve.

The heat source rod is loaded vertically into the hole, which is at the center of the radial TE leg samples. The bottom and top of the heat source rod are covered with foamed ceramic aluminum silicate fiber to reduce heat loss. A resistive joule thermal surrogate is used in the micro-RTG to simulate a radioactive fuel pellet for experimental research. The power range of 0–1.5 W represents the multiple heat-source columns. The experimental heat source covers the thermal power range of the above typical radioisotope heat source. Thermocouples are placed on the hot and cold sides of the prototype to monitor ΔT across the device. The micro-RTG is connected to a semiconductor characteristic parameter analyzer.

Table 1 Single-layer module thermoelectric-conversion electrical performance parameters

P_{th} (W)	I_{sc} (mA)	V_{oc} (mV)	P_{max} (μW)
0.5	0.350	30.005	2.613
1	0.643	59.504	9.661
1.5	0.927	88.001	20.480

Table 2 Output performance comparison of the micro-RTG prototype

P_{th}	I_{sc} (mA)	V_{oc} (V)	P_{max} (μW)
^{3}H-Ti	0.085	0.113	1.97
$^{241}AmO_2$	0.150	0.212	7.03
$^{90}SrTiO_3$	0.453	0.668	75.93
$^{238}PuO_2$	0.551	0.815	114.38

3 Result and Discussion

Measurement results show that the internal resistance of the single-layer sample produced in this experiment is mainly controlled between 70 and110 Ω, indicating excellent electrical properties.

Figure 2a shows the statistical results of the internal resistance experiment. Compared with the unoptimized single-layer module, resistance is significantly reduced, and the distribution is more stable and concentrated, indicating higher suitability for multilayer connection. Table 1 and Fig. 2b show the performance of single-layer components with or without FPC optimization at different heat-source powers. The maximum output power (P_{max}) reaches 20 μW, and the V_{oc} is close to one hundred millivolts. Thus, we estimate that 10 layers of similar samples can be soldered in series with a V_{oc} of several hundred millivolts and a P_{max} in the order of one hundred microwatts. We have completed the COMSOL simulation and prototype test of the 10-layer RTG prototype. In the simulation results, the resistance is idealized as 484 Ω. Under the same conditions, the maximum output power and open-circuit voltage of the 10-layer RTG prototype should be approximately 10 times that of the single layer, which is 438.14 μW and 0.921 V (1.5 W heat source simulation results), respectively. Figure 3 and Table 2 show the test results of the 10-layer prototype. Compared with 10 times the single layer performance, the voltage and power loss are smaller. Compared with the simulation results, it is found that there is a difference of 11% with the voltage and a difference of 73% with the power, which shows that the Seebeck coefficient has no significant effect, and the internal resistance of the device is greatly affected by the actual process.

During soldering, the internal resistance of each layer increases the contact resistance by several to several tens of ohms, which is an improvement compared with the

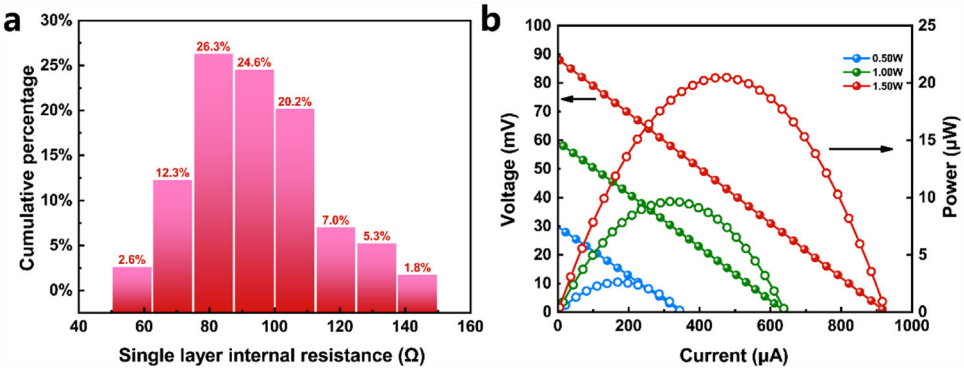

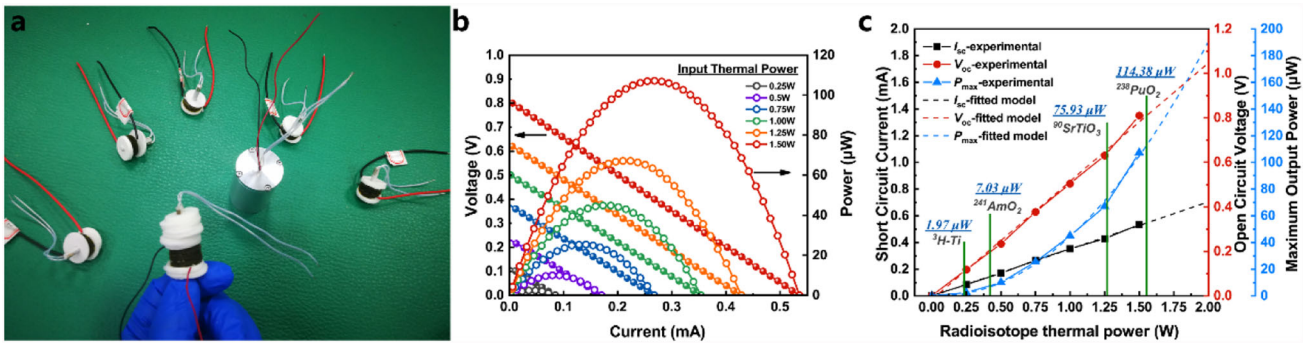

Fig. 2 **a** Component internal resistance and **b** IVP characteristics

Fig. 3 Electrical performance of assembled prototype RTG. **a** Assembled prototype. **b** and **c** Relationship between the heat source and electrical output

kΩ-level contact resistance in some related research work. Current–voltage-power curves (Fig. 3b) of the micro-RTG are obtained by changing the radioisotope heat-source power of the 10-layer prototype from 0.25 to 1.5 W. When this prototype is loaded with a heat source of 1.5 W, V_{oc} is 810.05 mV, P_{max} is 107.11 μW, and I_{sc} is 535.44 μA. With increased heating power, the output voltage and output power increase linearly and quadratically, respectively, along with the thermal power. The increase is much lower than the electromotive force, so the performance impact is small. In this work, the optimization of the electrode material also curbs the above effects.

The maximum thermal power of four typical radioisotope heat-source pellets with the same volume is shown in Fig. 3c. The relationship between the electrical parameters (V_{oc}, I_{sc}, and P_{max}) of the micro-RTG and the heat-source power is shown. The detailed electrical output performance of four radioisotope heat sources is shown in Table 2.

Two sets of integrated packaged generators are used in the application verification of wireless sensor networks, as shown in Fig. 4. The entire wireless sensor network system consists of multiple sets of independent modules, each of which has physical power (micro-RTG), DC converters, sensors, energy storage, RF transceivers, and so on. Two of the endpoints are powered by the micro-RTG. An access point is powered by the computer and reads the data. The three sets of components are identical except for the code executed by the microcontroller. It is transmitted by two sets of endpoints, and a set of access point receptions constitutes a complete minimum topology. The temperature and supply voltage parameters at the node were monitored intermittently for a long time. According to the needs of the application scenario and the chip reservation interface, digital signal sensors such as humidity, acceleration, and air pressure can be added to monitor key scientific indicators such as atmospheric water content and earthquake intensity on the target planet surface.

The micro-RTG may be deployed to work in different environments in the future. A 10-layer series RTG device is used to evaluate performance changes due to performance and ambient temperature effects. The internal resistance of the module increases by 12%. The performance parameters of the 10-layer prototype are related to the ambient temperature and heat source (as shown in Fig. 5). The R_{int}, V_{oc}, I_{sc}, and P_{max} of the 10-layer prototypes increase with increased temperature (− 30 to 120 °C). In the case of more considerable heat-source power, T_c is higher than the ambient temperature because of the insufficient length of the TE legs. When the experiment loads a low-power heat source, T_c is consistent with the ambient temperature due to the excessive length of the TE legs and the lower temperature heat-source surface, even without good heat dissipation. The output performance of the prototype changes obviously when

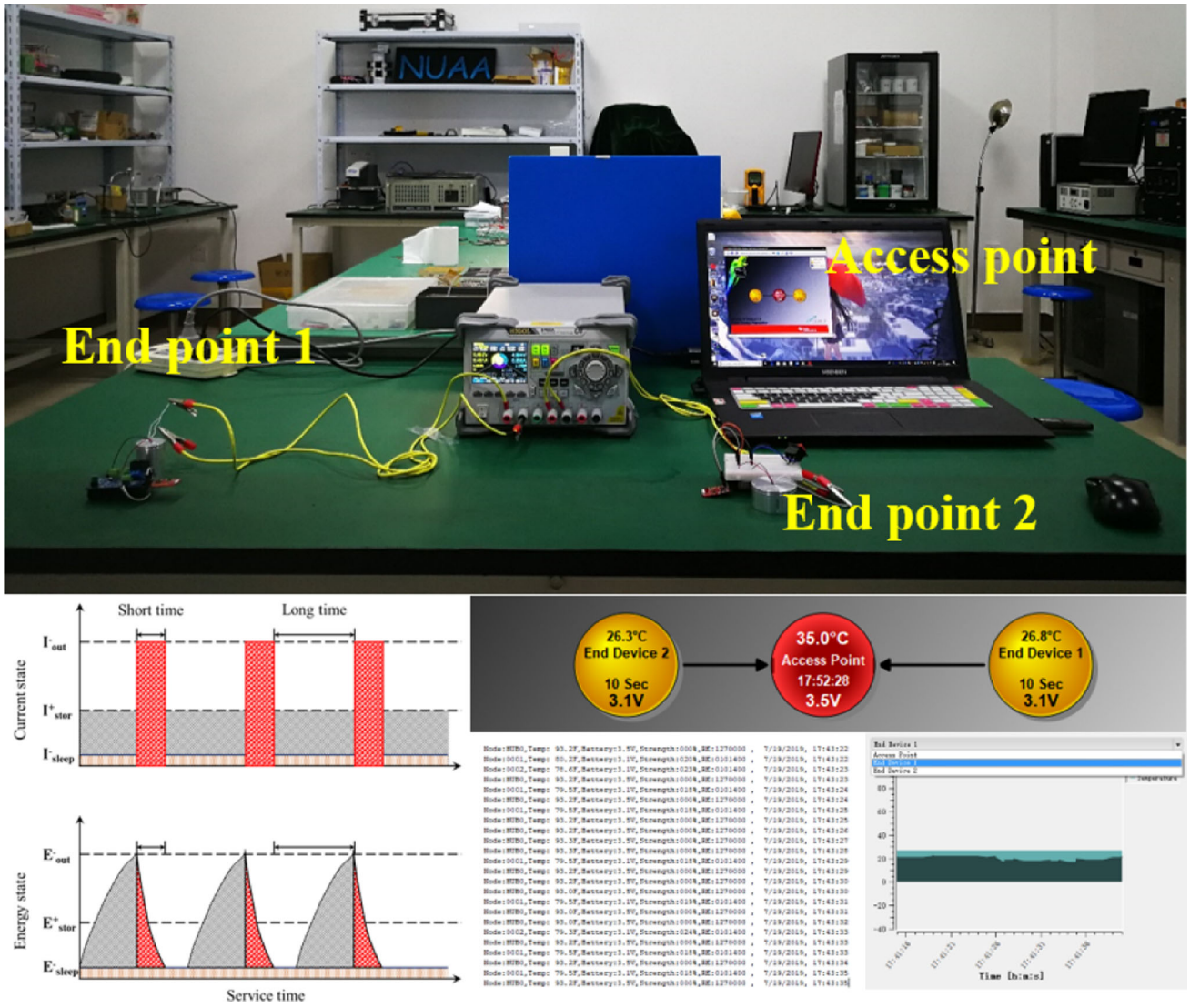

Fig. 4 Working state of a wireless sensor network test system with two endpoints

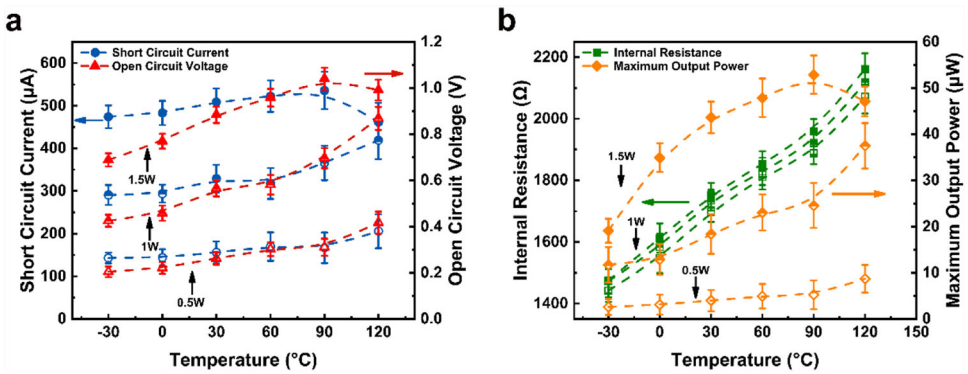

Fig. 5 Temperature dependence of the electrical performance of the integrated prototype. **a** Short-circuit current and open-circuit voltage. **b** Internal resistance and maximum output power

the high-power heat source and the high ambient temperature are loaded, which exceed the temperature dependence of the TE material. However, under the condition of low heat-source power, the increase in voltage is insignificant, whereas the increase in internal resistance is constant and the increases in current and P_{max} are small.

The open-circuit voltage decreased slightly, and the decrease in the performance of the control group did not

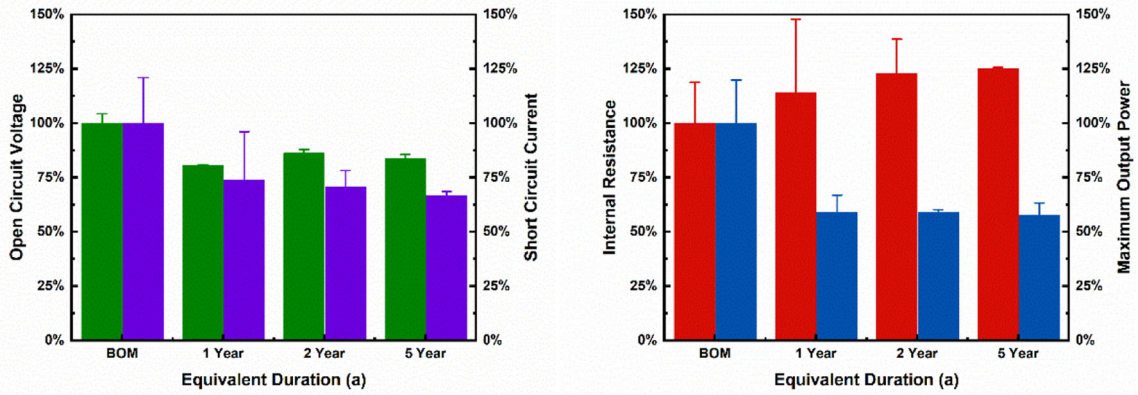

Fig. 6 Radiation effect of prototype component performance

have a linear or nonlinear relationship with the irradiation time, but a similar decrease in amplitude. Therefore, it is highly probable that thermoelectric material related parameters such as carrier concentration, mobility, etc., have a fixed loss to Seebeck coefficient. The internal resistance of the battery before and after the equivalent irradiation of Co-60 γ source is shown in Fig. 6. The internal resistance of the irradiated prototypes increased by 13–45% from 1 to 5 years and increased statistically with the increase of service time. Correspondingly, since the short-circuit current and the maximum output power are determined by the combination of the open-circuit voltage and the internal resistance, linear and quadratic correlation, respectively. However, often the limits of these two parameters are related to a high internal resistance module in the series device, so the error and uncertainty have a certain increase.

4 Conclusions

We develop a micro-stacked-integrated annular–radial RTG for the miniaturization, stability, and long-life power supply requirements of space micro scientific instruments. Manufacturing a highly integrated device is a challenge, and a new module component is designed for stacking to enhance power and voltage. The performance of the single-layer module is improved by screen printing on the FPC. When loaded with a $^{238}PuO_2$ radioisotope heat source, the 10-layer prototype supplies the P_{max} of 114.38 μW at 0.408 V, short-circuit current of 0.551 mA, and open-voltage of 0.815 V. The performance parameters of different radioisotope heat sources are compared, and data reference is made for the broad practical application of micro-RTGs. The stacked device and power management module drive a wireless sensor network with two nodes as a demonstration. In different temperature environments, current, voltage, and power increase with increased temperature. During the equivalent simulation of 5 years of service, the internal resistance of the integrated prototype increased by approximately 24.5%, the output voltage dropped by less than 20%, and the maximum output power attenuation was approximately 32.6%. This work provides new ideas and inspiration for space micropower supplies and is expected to provide long-term, stable, and reliable power supplies for space probes, deep-space wireless sensor networks, and monitoring electronics.

Acknowledgements This work is supported by the Shanghai Aerospace Science and Technology Innovation Project (Grant no. SAST2016112); the Funding of Jiangsu Innovation Program for Graduate Education (Grant no. KYLX16_0355).

References

1. Prelas M, Boraas M, De La Torre Aguilar F, Seelig JD, Tchouaso MT, Wisniewski D (2016) Nuclear batteries and radioisotopes. Springer, Cham, pp 286–287. https://doi.org/10.1007/978-3-319-41724-0
2. Prelas MA, Weaver CL, Watermann ML, Lukosi ED, Schott RJ, Wisniewski DA (2014) A review of nuclear batteries. Prog Nucl Energy 75:117–148. https://doi.org/10.1016/j.pnucene.2014.04.007
3. BairstowB, Lee YH, Oxnevad K (2018) Mission analysis for next-generation RTG study. In: IEEE aerospace conference proceedings, pp 1–19. https://doi.org/10.1109/AERO.2018.8396411
4. Bass JC, Allen DT (1999) Milliwatt radioisotope power supply for space applications. In: Proceedings, ICT'99 (Cat. No. 99TH8407) eighteenth international conference thermoelectr, pp 521–524. https://doi.org/10.1109/ICT.1999.843443
5. PustovalovA, Gusev V, Borshchevsky A, Chmielewski A (1999) Experimental confirmation of milliwatt power source concept. In: Proceedings ICT'99 XVIII international conference thermoelectric, pp 500–504
6. Khajepour A, Rahmani F (2017) An approach to design a90Sr radioisotope thermoelectric generator using analytical and Monte Carlo methods with ANSYS, COMSOL, and MCNP. Appl Radiat Isot. https://doi.org/10.1016/j.apradiso.2016.11.001
7. Abelson RD, Balint TS, Marshall KE, Noravian H, Randolph JE, Satter CM, Schmidt GR, Shirley JH (2004) Enabling exploration with small radioisotope power systems. Jet Propulsion Laboratory, National Aeronautics and Space, Pasadena, pp 2–5

8. Heshmatpour B, Lieberman A, Khayat M, Leanna A, Dobry T, El-Genk MS (2008) Special application thermoelectric micro isotope power sources. In: AIP conference proceedings AIP, pp 689–695. https://doi.org/10.1063/1.2845032
9. Roundy S, Steingart D, Frechette L, Wright P, Rabaey J (2004) Power sources for wireless sensor networks. Sens Netw. https://doi.org/10.1007/978-3-540-24606-0_1
10. Mohamed NS, Wright NG, Horsfall AB (2017) Self-powered X-Ray sensors for extreme environments. In: Proceedings IEEE sensors. https://doi.org/10.1109/ICSENS.2017.8234008.
11. BahramiP, Nesmith B, Carpenter K (2017) Milli-watt radioisotope power to enable small, long-term robotic "probe" space exploration. In: IEEE aerospace conference proceedings, pp 1–8. https://doi.org/10.1109/AERO.2017.7943899
12. MacDowall R (2018) Low-frequency radio observatory on the lunar surface (LROLS). In: Am. Astron. Soc. Meet. Abstr., pp 232
13. Gusev VV, Pustovalov AA, Rybkin NN, Anatychuk LI, Demchuk BN, Ludchak IY (2011) Milliwatt-power radioisotope thermoelectric generator (RTG) based on plutonium-238. J Electron Mater. https://doi.org/10.1007/s11664-011-1579-z
14. Selvan KV, Hasan MN, Mohamed Ali MS (2018) Methodological reviews and analyses on the emerging research trends and progresses of thermoelectric generators. Int J Energy Res 43:113–140
15. Fang H, Popere BC, Thomas EM, Mai CK, Chang WB, Bazan GC, Chabinyc ML, Segalman RA (2017) Large-scale integration of flexible materials into rolled and corrugated thermoelectric modules. J Appl Polym Sci. https://doi.org/10.1002/app.44208
16. Yuan Z, Tang X, Liu Y, Xu Z, Liu K, Zhang Z, Chen W, Li J (2017) A stacked and miniaturized radioisotope thermoelectric generator by screen printing. Sens Actuators A Phys 267:496–504. https://doi.org/10.1016/j.sna.2017.10.055
17. Yuan Z, Tang X, Xu Z, Li J, Chen W, Liu K, Liu Y, Zhang Z (2018) Screen-printed radial structure micro radioisotope thermoelectric generator. Appl Energy 225:746–754. https://doi.org/10.1016/j.apenergy.2018.05.073
18. Yuan Z, Tang X, Liu Y, Xu Z, Liu K, Li J, Zhang Z, Wang H (2019) Improving the performance of a screen-printed micro-radioisotope thermoelectric generator through stacking integration. J Power Sour 414:509–516